Near-infrared light activatable hydrogels for metformin delivery

Li Chengnan, Quentin Pagneux, Anna Voronova, Alexandre Barras, Amar Abderrahmani, Valérie Plaisance, Valérie Pawlowski, Nathalie Hennuyer, Bart Staels, Lea Rosselle, et al.

TOC image

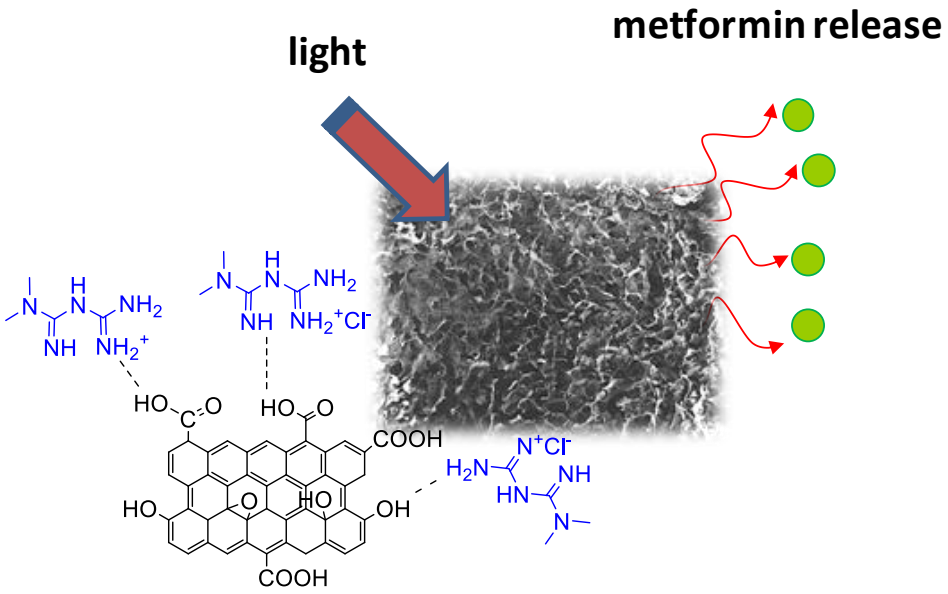

Near-Infrared Light activatable hydrogels for metformin delivery

Chengnan Li,[1,2] Quentin Pagneux,[1] Anna Voronova,[1] Alexandre Barras,[1] Amar Abderrahmani,[1] Valérie Plaisance,[1] Valerie Pawlowski,[1] Nathalie Hennuyer,[3] Bart Staels,[3] Lea Rosselle,[1,4] Nadia Skandrani,[4] Musen Li,[2] Rabah Boukherroub[1*] and Sabine Szunerits[1*]

[1] *Univ. Lille, CNRS, Centrale Lille, ISEN, Univ. Valenciennes, UMR 8520 - IEMN, F-59000 Lille, France*

[2] *Key Laboratory for Liquid-Solid Structural Evolution and Processing of Materials (Ministry of Education), Shandong University, Jinan 250061, China*

[3] *Univ. Lille, Inserm, CHU Lille, Institut Pasteur de Lille, U1011 - EGID, F-59000 Lille, France*

[4] *TISSUEAEGIS SAS, 14E rue Pierre de Coubertin 21000 Dijon, France*

Abstract

Drug loaded hydrogels have proven to be versatile controlled-release systems. We report here on heat active hydrogels' formation by mixing graphene oxide (GO) or carboxyl enriched reduced graphene oxide (rGO-COOH) with metformin hydrochloride, an insulin sensitizer drug currently used as first line therapy to treat patients with type 2 diabetes. The driving forces of the gelation process between the graphene-based nanomaterial and metformin are hydrogen bonding and electrostatic interactions, weakened at elevated temperature. Using the excellent photothermal properties of the graphene matrixes, we demonstrate that these supramolecular drug reservoirs can be photothermally activated for transdermal metformin delivery. A sustained delivery of metformin was achieved using a laser power of 1 W cm^{-2}. *In vitro* assessment of the key target Glucose-6 Phosphatase (G6P) gene expression using Human hepatocyte model confirmed that metformin activity was unaffected by photothermal activation. *In vivo*, metformin was detected in mice plasma at 1h post-activation of the metformin loaded rGO-COOH gel.

Keywords: metformin, graphene; photothermal; transdermal; *in vitro* and *in vivo* assays

[*] To whom correspondence should be send to: sabine.szunerits@univ-lille.fr

1. Introduction

Advancements in materials science have impacted positively to the development of on-demand drug delivery.[1] Among the various external stimuli, the high spatial and temporal resolution of near-infrared (NIR) light, has shown to be highly beneficial for drug delivery.[2-5] NIR-triggerable drug delivery platforms are largely based on NIR absorbing nanomaterials, notably on reduced graphene oxide (rGO) based matrixes.[6-9] The effectiveness of rGO as NIR-absorbing photothermal agent compared to other carbon allotropes is due to the rapid light-to-heat conversion of rGO under low-power NIR irradiation. This has made rGO preferential filler in polymeric blends and composite hydrogels.[10-15] Next to efficient drug delivery, near-infrared light has also been considered as external trigger to enhance transdermal drug delivery.[4, 6, 7, 16, 17] Transdermal drug delivery systems are more and more considered for personalized medicine and are a pain free alternative to hypodermic injections.[18, 19]

In this paper the formulation of light responsive transcutaneous patch, based on gelation between rGO and metformin will be shown as well as its use for the transdermal delivery of metformin.

Metformin hydrochloride is a commonly used anti-hyperglycemic agent and represents currently the first line drug in the management of Type 2 diabetes.[20] While metformin is conveniently administered orally in the form of tablets, some patients experience side effects including nausea, abdominal pain and indigestion, often leading to a discontinuation of the treatment. Furthermore, metformin exhibits an unfavorable pharmacokinetics profile, with low and variable oral bioavailability (50-60%) and a biological half-life time in the range of 0.9-2.6 h.[20, 21] Therefore, frequent applications of high doses of metformin (0.5- 2g twice daily) are required for an effective treatment

To overcome these limitations, transdermal delivery of metformin has been identified as an effective alternative.[4, 22-26] The transdermal administration route allows metformin to be delivered into the body bypassing the gastrointestinal tract and avoiding many of the unpleasant side effects. Additionally, the enhanced bioavailability of metformin allows reducing the administered daily dose amount and its frequency. The transdermal delivery of metformin is currently limited to the use of thermo-responsive microneedles, where metformin is released upon needle melting,[4, 22, 25, 26] and the use of hydrogel-based microneedles.[24] The advantage of hydrogel-based microneedles over thermo-responsive microneedles is that once applied to the skin they can be withdrawn and remain intact. Onto this microneedles metformin reservoirs were integrated to have access to a sufficient amount of metformin.

In this work we investigate the potential of thermo-responsive metformin gels as a transdermal controlled release system. Hydrogels are extensively used in controlled-release systems due to their hydrophilic character and good biocompatibility. These systems are commonly prepared using self-assembly processes and benign conditions in contrast to polymeric gels for which toxic photo-initiators and cross-linkers are employed for their formation.[7, 27] We show here that simple mixing of metformin with graphene based derivatives, such as graphene oxide (GO) or carboxylated reduced graphene oxide (rGO-COOH), as cross-linkers in a volume ratio of 1/9 results in metformin gel formation. The gelation process is believed to be driven mainly by hydrogen bonding and electrostatic interactions. Photothermal activation of GO/metformin and rGO-COOH/metformin gels results in a stepwise dissolution of the gel and release of active metformin. *In vitro* assessment of the key target Glucose-6 Phosphatase (G6P) gene expression using Human hepatocyte model[28] confirmed that metformin activity[29] was unaffected by photothermal activation.

2. Experimental Section

2.1. Materials

Metformin hydrochloride, hydrazine hydrate ($NH_2NH_2{\bullet}H_2O$), sodium hydroxide (NaOH), chloroacetic acid (Cl-CH_2COOH), acetonitrile, potassium dihydrogen phosphate buffer (pH 6) and sodium dodecyl sulfate (SDS) were obtained from Aldrich. Kapton® HN polyimide foils (thickness of ~75 µm) were provided by DuPont (Circleville, OH, USA). Graphene oxide (GO) was purchased from Graphitene (UK).

2.2. Formation of reduced graphene oxide (rGO) and carboxylic acid enriched rGO (rGO-COOH)

The reduction of GO to reduced graphene oxide (rGO) was performed by adding hydrazine hydrate (0.1 mL, 6.42 mM) to 100 mL of GO aqueous suspension (3 mg mL^{-1}) in a round bottom flask and heated in an oil bath at 80 °C for 24 h. The product was isolated by filtration over a polyvinylidene difluoride (PVDF) membrane with a 0.45 µm pore size, washed copiously with Milli-Q water and vacuum dried for further use.

Carboxylic acid enriched GO (GO-COOH) was synthesized from GO.[30, 31] In short, sodium hydroxide (NaOH, 1.4 g) and chloroacetic acid (Cl-CH_2-COOH, 1 g) were added to 50 mL of GO (20 mg) aqueous solution and sonicated at 35 kHz for 2 h at 80 °C to convert hydroxyl groups present on GO to COOH via conjugation of acetic acid moieties and to partially reduce GO into rGO. The resulting rGO-COOH solution was quenched with HCl (20%), washed (four

times) with distilled water until neutral pH and purified by repeated rinsing/centrifugation (4500 rpm., 30 min) cycles.

2.3. Fabrication of metformin hydrogel

The metformin gel was fabricated by mixing GO or rGO-COOH (10 mg mL^{-1}) and metformin hydrochloride (10 mg mL^{-1}) at a volume ratio of 9:1 (v/v) and homogenized by sonication for 5 min prior to lyophilization for 12 h before use.

2.4. Metformin release into solution and quantification

Release experiments were performed into 1 mL deionized water under passive conditions (without any stimulation) and upon illumination of the metformin based gels using a 980 nm-continuous wave laser (Gbox model, Fournier Medical Solution) at 0.5-1.0 W cm^{-2}. The temperature changes were captured by an infrared camera (Thermovision A40) and treated using ThermaCam Researcher Pro 2.9 software. The released metformin concentration was determined by reversed phase-high performance liquid chromatography (RP-HPLC) on a Shimadzu LC2010-HT (Shimadzu, Tokyo, Japan) at a wavelength of 230 nm. The mobile phase is acetonitrile/potassium dihydrogen phosphate buffer pH 6.5 (34/66, v/v) and 3 mM SDS and was run at a flow rate of 0.3 mL min^{-1}. The reverse phase column was a 2.6 µm C18, 150×4.6 mm column (Interchim, Montluçon, France).

2.5. Characterization

Scanning Electron Microscopy (SEM) images were obtained using an electron microscope ULTRA 55 (Zeiss) equipped with a thermal field emission emitter and three different detectors (Energy selective Backscattered Detector with filter grid, high efficiency In-lens Secondary Electron Detector and Everhart-Thornley Secondary Electron Detector).

UV/Vis Absorption spectra were recorded using a Perkin Elmer Lambda UV-Vis 950 spectrophotometer in a 1-cm quartz cuvette. The wavelength range was 200 - 1100 nm.

X-ray photoelectron spectroscopy (XPS) was recorded using ESCALAB 220 XL spectrometer from Vacuum Generators featuring a monochromatic Al Kα X-ray source (1486.6 eV) and a spherical energy analyzer operated in the CAE (constant analyzer energy) mode (CAE = 100 eV for survey spectra and CAE = 40 eV for high-resolution spectra), using the electromagnetic lens mode. The angle between the incident X-rays and the analyzer is 58° and the detection angle of the photoelectrons is 30°.

Micro-Raman spectroscopy measurements were performed on a Horiba Jobin Yvon LabRam high resolution micro-Raman system combined with a 473 nm (1 mW) laser diode as excitation source. Visible light is focused by a 100× objective. The scattered light is collected by the same objective in backscattering configuration, dispersed by a monochromator with 1800 mm focal length and detected by a CCD camera.

Zeta-potential measurements were performed using a Zeta-sizer Nano-ZS (Malvern Instruments Inc. Worcestershire, UK). Samples were diluted to 10 µg mL^{-1} and measured in Milli-Q water at different pH.

2.6. Skin permeation experiments

Skin permeation studies were performed using fresh mice skin. For this, mice C57BL/6 were anaesthetized with isoflurane, shaved with an electric shaver (Philips Series 7000) and further treated with a depilatory cream (Veet) for 1.5 min. Then mice were killed by cervical dislocation and the skin from the back of the mice was cut into pieces of at least 20 mm in diameter and preserved in Dulbecco's modified Eagle medium (DMEM) supplemented with gentamicin (0.4%).

Static Franz diffusion cells (Proviscin, France) exhibiting an effective area of 0.785 cm^2 were used for skin permeability tests. After filling the receptor compartment with degassed phosphate buffer saline (PBS, pH = 7.4) the solution was maintained at 32 °C using a circulating bath (Julabo) and stirred with a magnetic stirring bar at around 500 rpm. Freshly cut mouse skin was clamped between the donor and the receptor compartment (8 mL), pre-incubated for 20 min, and wetted with 30 µL of a glycerin solution (50%) to insure contact between the gel and the skin. The metformin gels were applied to the skin and the passive permeability and light activated permeability (980 nm laser, power densities between 0.5-1.0 W cm^{-2}) were evaluated. At determined time intervals, 500 µL aliquots of diffused solution were removed from the receptor compartment and analysed using HPLC. After each sampling, an equal volume of fresh diffusion medium was added to the receptor compartment to maintain a constant volume. All experiments were performed in triplicates.

To estimate the amount of metformin trapped in the mice skin, the skin was added into a water/ice mixture for 10 min and sonicated in the presence of ZrO_2 beads (4 mm in diameter), before being centrifuged for 30 min at 13.500 rpm using an ultracentrifuge (Midi Scanfuge ORIGIO). The liquid phase was collected and filtrated through a 0.1 µm Nylon filter (Whatman Puradisc 13 mm) and the amount of metformin was determined. The metformin flux (J, µg cm^{-2} h^{-1}) was determined according to equation (1):

$$J = m/A \quad (1)$$

with m being the linear slope of the cumulative metformin amount *versus* time curves in equilibrium conditions (µg h^{-1}), and *A* is the surface of the membrane of the Franz cell (0.785 cm^2).

2.7. Skin staining

For skin staining experiments an *ex vivo* human skin model (HypoSkin®, Genoskin SAS, Toulouse, France) was used. The rGO/metformin gels were deposited onto the skin and irradiated for 10 min at 0.5, 0.7 and 1 W cm^{-2}. Part of the skin was then fixed with formaldehyde (4 %), embedded in paraffin and sectioned (5 µM pieces in thickness). Tissue sections were stained with hematoxylin and eosin (H&E) to observe the tissue structure.

2.8. *In vitro* studies

In vitro assessment of metformin activity was performed using the Immortalized Human Hepatocytes (IHH) as relevant Human hepatocyte cell model as they retain features of normal hepatocytes.[28] IHH cells (maintained at passages 25-35) were cultured in Williams E medium (Invitrogen) containing 11 mM glucose and supplemented with 10 % fetal calf serum (FCS; Eurobio), 100 U/mL penicillin, 100 µg/mL streptomycin, 20 mU/mL insulin (Sigma-Aldrich) and 50 nM dexamethasone (Sigma-Aldrich). The activity of metformin when heated at 45 °C, 55 °C and 65 °C was assessed by monitoring the glucose-6-phosphatase catalytic (G6PC) gene expression from IHH cells (4×10^5 cells) cultured in 12-well plates in a Dulbecco's Modified Eagle Medium (DMEM; Invitrogen) supplemented with 5 mM glucose, 2 % FCS, 100 U/mL penicillin, 100 µg/mL streptomycin containing either PBS (Control) or 5 mM heated metformin for 24 h. Total RNA was extracted from IHH cells according to the manufacturer's protocol (RNeasy Lipid Tissue Kit, Qiagen). The RNA purity and concentration were determined by RNA Integrity Number (RNA 6000 Nano Kit, 2100 Bioanalyser, Agilent). Total RNA was transcribed into cDNA as described before.[28] Each cDNA sample was quantified by quantitative real-time polymerase chain reaction using the fluorescent TaqMan 5′-nuclease assays or a BioRad MyiQ Single-Color Real-Time PCR Detection System using the BioRad iQ SYBR Green Supermix, with 100 nM primers and 1 µL of template per 20 µL of PCR and an annealing temperature of 60 °C. Gene expression analysis was normalized against TATA box Binding Protein (*TBP*) expression or 60S acidic ribosomal protein P0 (*RPLP0*). Primers for human *RPLP0* (sense 5′- ACCTCCTTTTTCCAGGCTTT -3′; antisense 5′-

CCCACTTTGTCTCCAGTCTTG -3′); Primers for human G6PC (sense 5’-AGACTCCCAGGACTGGTTCA-3’; antisense 5’-ACAGGTGACAGGGAACTGCT-3’); Primers for human *TBP* (sense 5’- GAACCACGGCACTGATTTTC-3’ and antisense 5’-CCCCACCATGTTCTGAATCT-3’)

2.9. *In vivo* studies

Mice were acclimatized for 7 days prior to *in vivo* studies. The animals were shaved the day before the experiment by using depilatory cream and separated into four groups (n=3 per group). In the oral control group, animals receivedal solution of carboximetilcelulosa (CMC) (0.5 % w/v). In the second group, mice were fed with CMC (0.5 %) and metformin (200 mg/kg) based on individualized mice weight. The third one are animals where metformin was injected subvutaneously (200 mg/kg). The forth group was the rGO-COOH/metformin treatment group where a gel with 2g metformin was activated for 10 min at 0.7 W cm^{-2}.

To facilitate the patch application, mice were sedated with isoflurane (2-4 % v/v in air) and the patch placed to the back of the mice. To secure the patch in place, an occlusive dressing layer was placed on the top and Micropores tape was used to wrap the back of the animals.

Blood samples were taken *via* the Retro Orbital sampling method at a pre-defined time with a maximal of 210 µL collection at each sampling spot into heparinized tubes. The samples were analysed by HPLC.

All *in vivo* experiments are conducted in accordance with the policy of the European Convention for the protection of vertebrate animals with implementation of the Principe of the 3Rs (replacement, reduction and refinement). Approval for animal experiments was obtained from Institute Pasteur Lille, France.

2.10. Quantification of metformine in *in vivo* samples

Before metformin quantification in blood, the collected whole blood samples (200 µL) were centrifuged at 3000 rpm for 20 min at 4°C. 100 µL of plasma were collected and diluted with water (400 µL) and vortexed for 5 sec. Then acetonitrile (500 µL) was added and vortexed for 30 sec, before being cenrifugated at 1000 rpm for 10 min at RT. The supernatant was collected in a new tube and the precipitate dissolved in 500 µL of acetonitrile, sonicated for 3 min and recentrifuged at 1000 rpm for 10 min at RT. The supernatant was collected and mix to the first supernatants. Formed white precipitate was discarded and the supernatant evaporated. The sample is taken up in 1 mL water and s injected into the HPLC column. Quantification was performed using reversed-phase HPLC. Chromatographic separation was achieved using

column C18 fitted with a UV detector at 235 nm. The mobile phase is 50mM of KH_2PO_4 and 3 mM of SDS mixed in water/acetonitrile (34/66%). The column temperate was 25°C and the flow rate was 0.3 mL/min with an injection volume of 10 µL.

3. Results and discussion

3.1. Metformin hydrogels using graphene oxide (GO) as a cross-linker

Figure 1A depicts the formation of a metformin hydrogel, using graphene oxide (GO) as a cross-linker. The hydrogel is obtained under mild conditions by mixing GO/metformin in a weight ratio of 10/1. **Figure 1B** exhibits the SEM images at different magnifications of a lyophilized sample, revealing a porous structure with a pore size of about 10±5 µm. **Figure 1C** shows the characteristic Raman features of GO and the GO/metformin gel with the G band centered at around 1585 cm^{-1} corresponding to the in-plane sp^2 C-C stretching, and the D band at 1350 cm^{-1} due to defects in the GO structure. The ratio of I_D/I_G is 0.76 for GO and increased to 0.93 for GO-metformin arguing for an increase in defects due to the gelation process. The UV/Vis spectrum of GO/metformin (**Figure 1D**) comprises a strong absorption band in the ultraviolet at 233 nm, characteristic of metformin as well as contributions from GO (π-π* of the aromatic bonds at ~230 nm and a shoulder at ≈310 nm due to n-π* of C=O),[32] along with a slight increase of the absorption tail until the near-infrared region. The photothermal heating curve of GO/metformin is in accordance with the UV/Vis spectrum; the hydrogel achieves a moderate heating capacity at 980 nm (**Figure 1E**), resulting in a solution temperature of 41°C after 10 min irradiation.

While the XPS survey spectrum of GO shows only the presence of C and O with a C/O ratio of 2.1, GO/metformin (**Figure 1F**) shows in addition the presence of nitrogen of 5.4 at. % . The C_{1s} high resolution spectrum of GO/metformin displays bands at 284.4, 285.0, 286.6, 288.3 eV corresponding to C=C (sp^2), C-C (sp^3)/C-H, C-O/C-N, and C=O, respectively (**Figure 1G**).[33] As metformin lacks aromatic structures, strong hydrogen bonding and electrostatic interactions between GO and metformin are believed to drive the gelation process.[15]

(A)

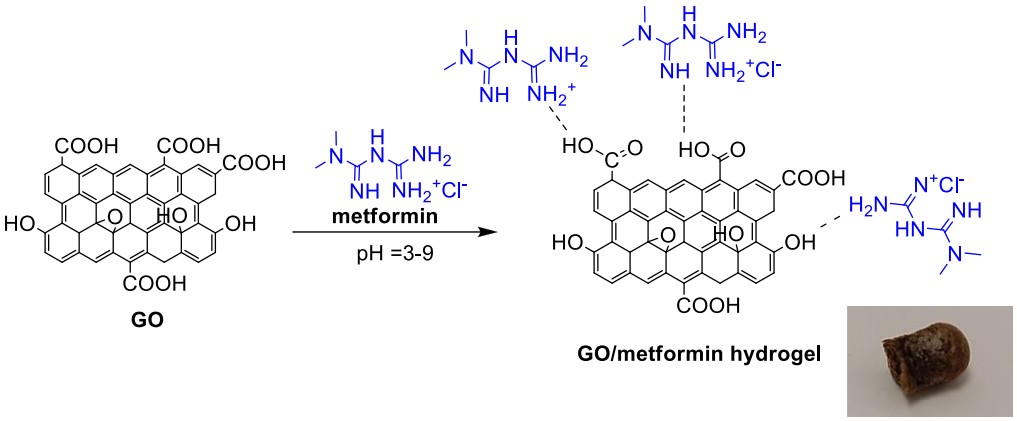

(B)

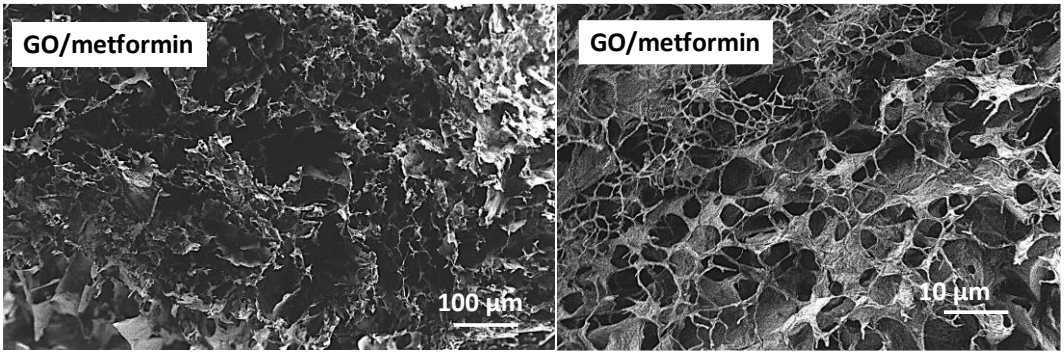

(C)

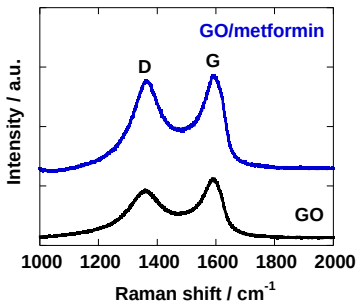

(D)

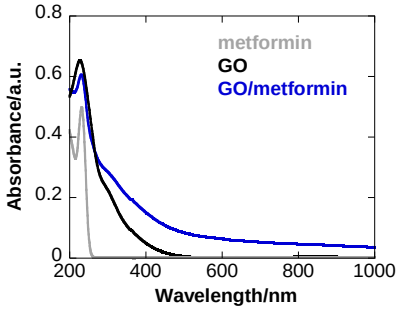

(E)

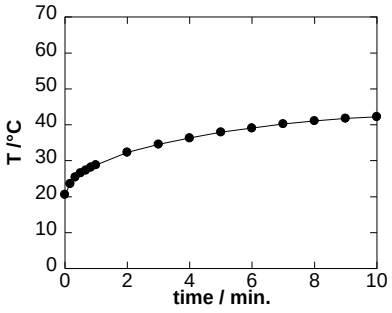

(F)

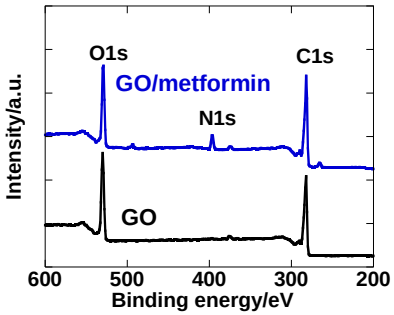

(G)

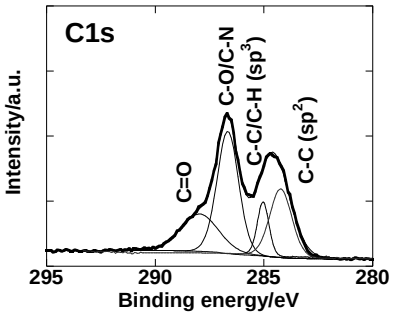

Figure 1: (A) Graphene oxide (GO) based metformin encapsulated hydrogel together with photographic image of the lyophilized gel; (B) SEM images of lyophilized GO/metformin gel;

(C) Raman spectra of GO (black) and GO/metformin (blue); (D) UV/Vis of metformin (grey), GO (black) and GO/metformin (blue); (E) Change of temperature upon laser irradiation at 980 nm (1 W cm^{-2}) for 10 min; (F) XPS survey spectra of GO (black) and GO/metformin (blue); (G) C1s high resolution spectrum.

The stability of the GO/metformin hydrogel is strongly pH dependent (**Figure 2A)**.[15] Immersion of GO/metformin gel into NaOH (0.1 M, pH 12) results in a fast decomposition of the gel most likely due to the deprotonation of –COOH groups of GO under basic conditions, decreasing hydrogen bonding occurrence with metformin. With a pKa of 12.4 for metformin breaking of electrostatic interactions with negatively charged GO can occur as well. Lowering the pH reduces the degree of negative charge on GO (**Figure 2B**) and electrostatic interaction; however hydrogen-bonding between GO and metformin limits the full collapse of the GO/metformin hydrogel until pH 3. The release profile of metformin at ambient conditions (T=23°C) is in accordance with the stability of the GO/metformin gels (**Figure 2C**): a release of about 5 µg mL^{-1} between pH 3 and 9, while the instability of the gel at pH 12 results in a complete release of metformin as expected. This high pH is, however, not adequate for most medical applications.

The effect of photothermal heating on metformin release from the gels immersed in PBS (pH 7.4) was further assessed. As depicted in **Figure 2D**, photothermal heating using a laser density of 1 W cm^{-2} (corresponds to a steady-state temperature of 47°C) leads to improved metformin release from the GO/metformin gel, where about 12 µg (12%) of metformin is released per laser activation, while without activation a total amount of 9 µg (9%) is released in the first two hours and then remains constant. The amount of metformin released is comparable to other reports using NIR melting microneedles with metformin release between 12-24%.[22, 25]

(A) **(B)** **(C)**

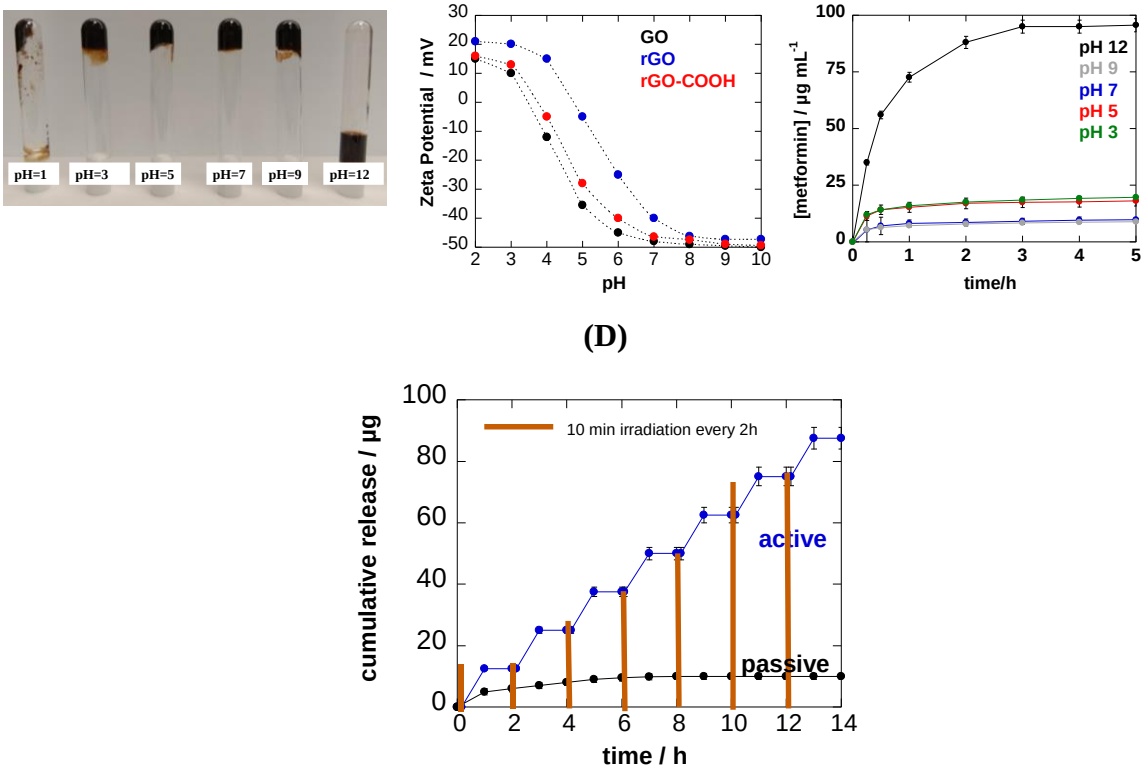

Figure 2: (A) GO/metformin gel formation as a function of solution pH; (B) Zeta potential of Go, rGO and rGO-COOH as a function of solution pH; (C) Release profiles of metformin from freeze-dried samples upon immersion into solutions of different pH (3, 5, 7, 9, and 12). The data points are averaged over three parallel experiments; (D) Metformin release from GO/metformin gel into PBS (pH 7.4) upon photothermal irradiation of the GO/metformin gel at 980 nm (10 min at 1 W cm^{-2} every 2 h) in comparison to passive release.

3.2. Metformin hydrogels using reduced graphene oxide (rGO-COOH) as a cross-linker

We were intrigued if replacing highly oxidized GO, with known suboptimal absorption of NIR light, with reduced GO (rGO) would allow to optimize metformin release. Partial restoration of the aromatic network in rGO affords a significant increase in NIR absorbance and rGO has become of particular interest as a highly effective photothermal agent.[34] However, as can be seen in **Figure 3**, the crosslinking properties of rGO with metformin are too weak due to absence of hydroxyl and carboxylic functions on rGO needed for hydrogen bonding formation and decreased electrostatic interactions with metformin (**Figure 2B**) at more acidic pH.

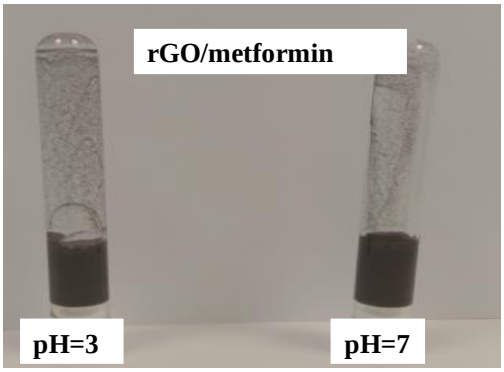

Figure 3: (A) rGO/metformin gel formation as a function of solution pH

Therefore, to enrich rGO with carboxylic acid groups, we synthesized water dispersible rGO-COOH. The synthetic procedure is based on the reaction of GO with chloroacetic acid under strong basic conditions (**Figure 4A**).[31] Furthermore, by performing the carboxylation reaction at elevated temperature, a partial reduction of GO was achieved, as evidenced by the increased absorption tail in the NIR region of the UV/Vis spectrum (**Figure 4B**). XPS analysis confirmed the formation of rGO-COOH/metformin (**Figure 4C**) by the presence ofw5.3 at % N next to C and O. The high resolution C1s spectrum of rGO-COOH/metformin shows bands at 284.6, 286.6, 288.5 and 292.7 eV corresponding to C-C, C-O/C-N, C=O and O-C=O (**Figure 4D**).

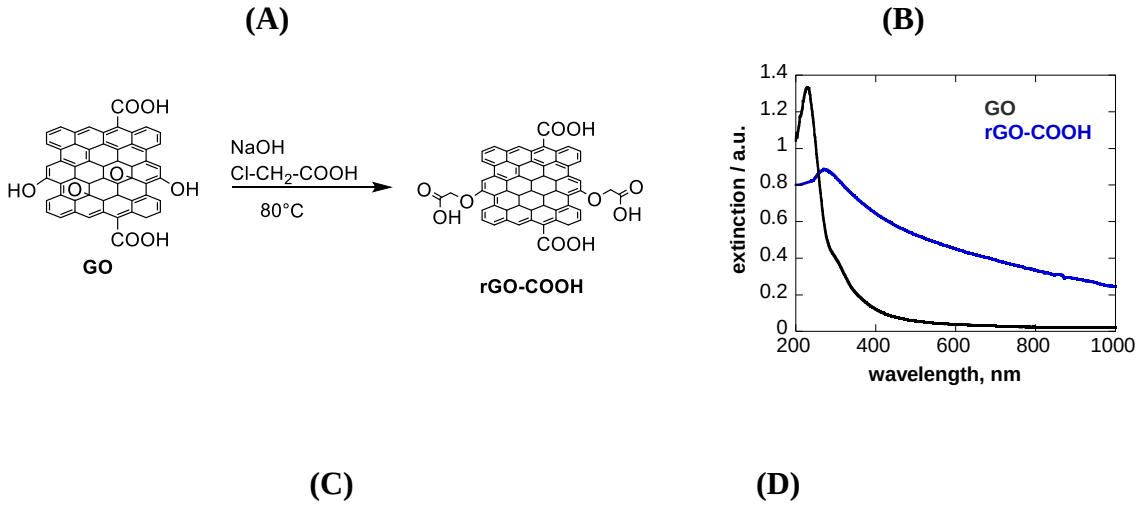

(C) **(D)**

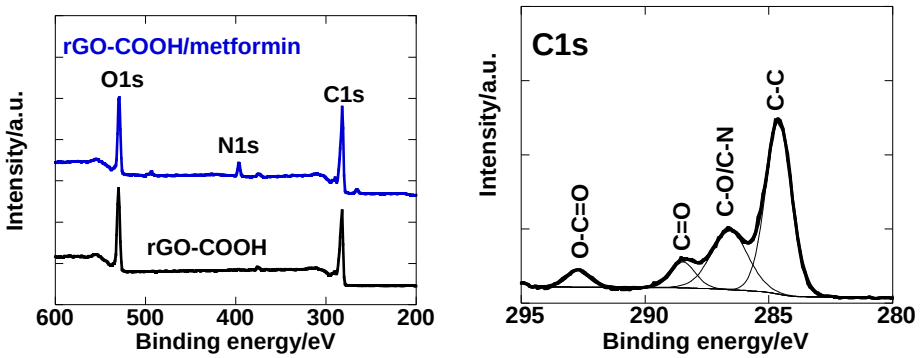

Figure 4: (A) Synthetic procedure for the preparation of rGO-COOH; (B) UV/Vis spectrum of GO and rGO-COOH; (C) XPS survey spectrum for rGO-COOH (black) and rGO-COOH/metformin (blue); (D) C1s high resolution XPS spectrum of rGO-COOH/metformin.

The gelling process of rGO-COOH with metformin is also pH dependent with stable gels obtained at pH< 7 (**Figure 5A**). The formed gel has a porous structure with an average pore size of 25 ±10 nm (**Figure 5B**), somehow larger than that of GO/metformin. Using rGO-COOH as a cross-linker rather than GO significantly improves the photothermal properties of the rGO-COOH/metformin gel (**Figure 5C)** due to favorable light-matter interaction of rGO-COOH, showing stronger absorption in the near infrared compared to GO (**Figure 4B**).

The better heating ability of rGO-COOH results in an increased metformin release from the gel upon laser activation at 1 W cm^{-2} (corresponding to a steady-state temperature of 61°C) where about 25 µg (21%) of metformin is released per laser activation (resulting in a total of 75 µg for 3 laser activation cycles of 10 min each). Passive release is increased due to the larger pore size attaining a total amount of 11 µg (11%) in the first two hours and then remains constant (**Figure 5E**).

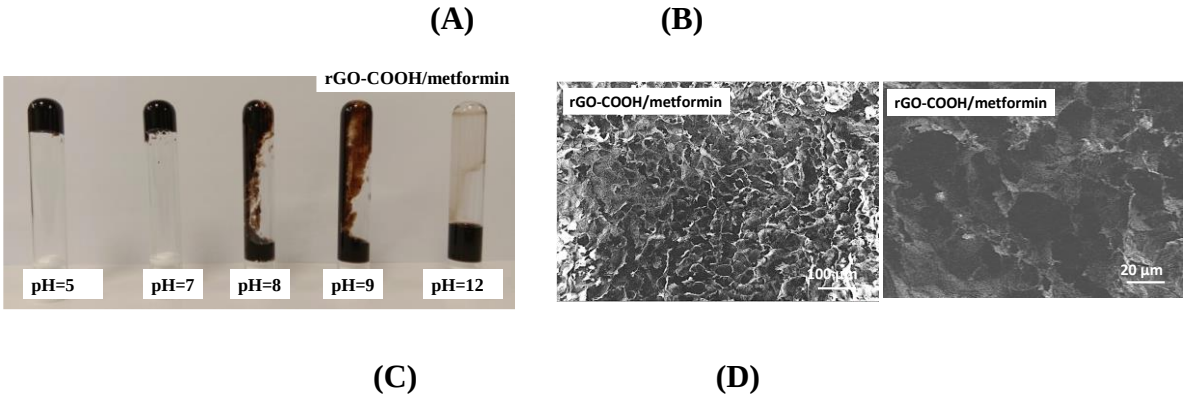

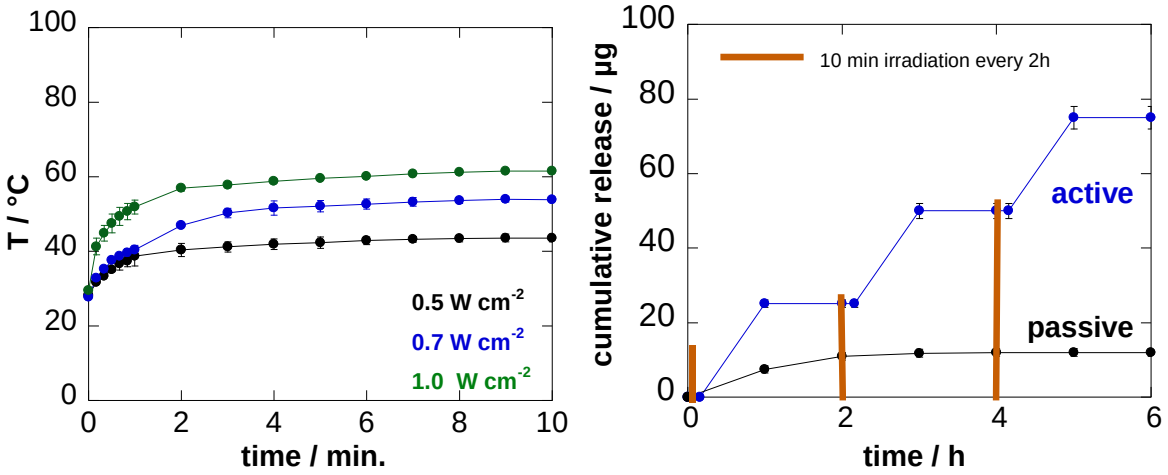

Figure 5: (A) Photographs of rGO-COOH/metformin gels at different pH; (B) SEM images of a rGO-COOH/metformin gel; (C) Change of temperature upon laser irradiation at 980 nm at 0.5, 0.7 and 1.0 W cm^{-2} laser power for 10 min; (D) Metformin release from a rGO-COOH/metformin gel into PBS (pH 7.4) upon photothermal irradiation of the GO/metformin gel at 980 nm (10 min at 1 W cm^{-2} every 2h) in comparison to passive release.

3.3. NIR light triggered transdermal metformin release

The rGO-COOH/metformin heatable hydrogel is further implemented in *ex vivo* transdermal drug delivery studies using mice skin in Franzen diffusion cells (**Figure 6A**). **Figure 6B** represents the cumulative permeation profile of metformin from rGO-COOH/metformin gels (500 µg) passively and under the impact of one-time NIR laser irradiation at 1 W cm^{-2} (corresponding to about 61 °C) and at 0.7 W cm^{-2} (corresponding to about 54 °C). After 6 h permeation, 80±8 µg cm^{-2} (16% of total patch as determined by HPLC, 1 W cm^{-2}) and 56±5µg cm^{-2} (12%, 0.7 W cm^{-2}) metformin had diffused through the skin. The combined metformin delivery for a day is 319±8 µg cm^{-2} (64%, 1 W cm^{-2}) and 222±10 µg cm^{-2} (45%, 0.7 W cm^{-2}). The passive release after 24 h corresponds to 50±5 µg cm^{-2} (10%). The efficiency of thermal-induced transdermal metformin delivery of rGO-COOH/metformin gel is competitive with the hydrogel microneedles reported recently by Migdadi et al., reaching a release percentage of 12.94±2.96% and 37.53±3.17% after 6 and 24 h, respectively.[24] About 5-30 µg (5-6%) of metformin was further found to be trapped in the skin (**Figure 6C**).

To ensure that NIR laser irradiation did not alter the activity of metformin, *G6PC* mRNA in human IHH hepatocytes cells exposed to metformin photothermally heated at 45 °C, 55 °C and 65 °C, which approximately correspond to 0.5, 0.7 and 1.0 W cm^{-2}, was measured. Reduction of the *G6PC* expression in hepatocytes, leading to diminished gluconeogenesis, partly accounts

for the improved insulin sensitivity and the antidiabetic effect of metformin.[29] As previously observed, exposure of IHH cells to native metformin results in drastic reduction of the *G6PC* expression (**Figure 6D**). The effect of metformin heated at 45 °C, 55 °C and 65 °C on the decrease of *G6PC* mRNA level was comparable to that of caused by native metformin (**Figure 6D**), indicating that the laser irradiation enabling the transdermal metformin delivery does not affect the drug activity.

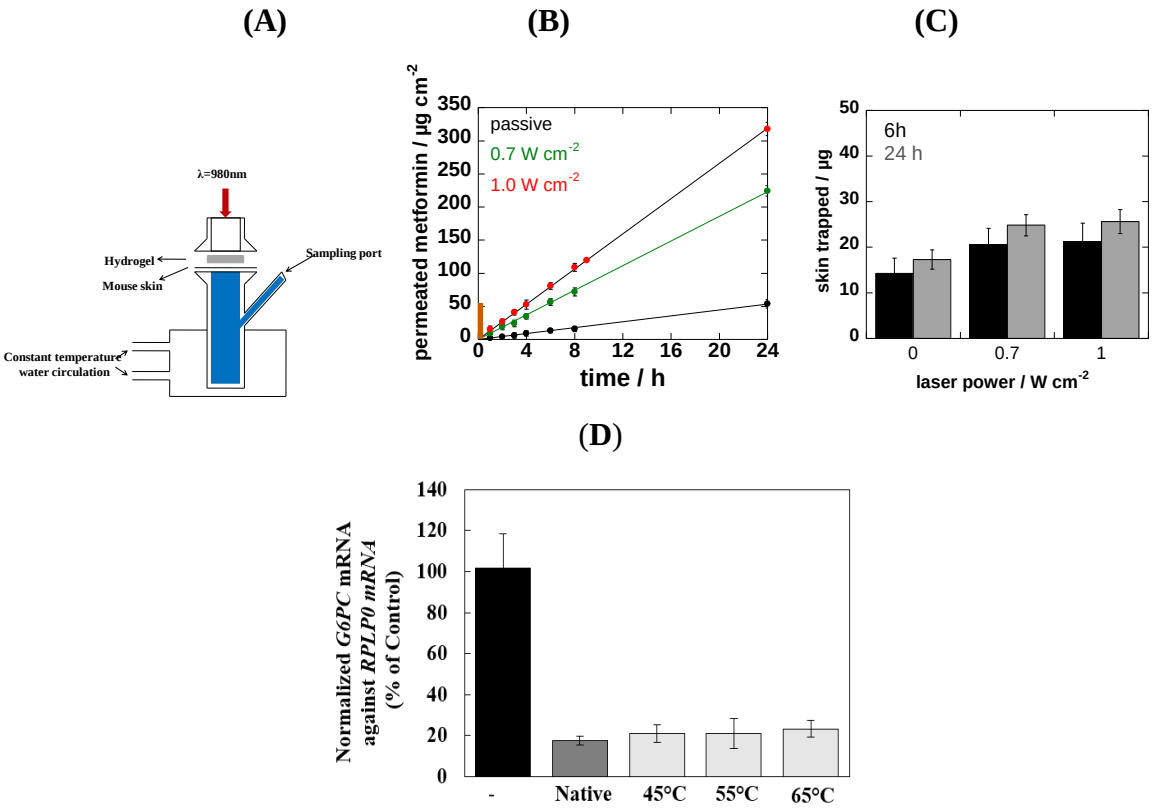

Figure 6: *Ex vivo* permeation profiles of metformin assessed using Franz diffusion cells: (A) Experimental ex-vivo set up; (B) rGO-COOH/metformin gel of 500 µg metformin activated one time for 10 min at 0.7 W cm^{-2} (green) or 1.0 W cm^{-2} (red) as well as without activation (black); (C) amount of metformin trapped in the skin; (D) The *Glucose 6 Phosphatase Catalytic (G6PC)* mRNA level of human IHH hepatocyte cells exposed to heated (45, 55 and 65 °C) and native metformin for 24 h. The *G6PC* mRNA was normalized against the *RPLP0* mRNA. Similar result was found upon normalization against *TBP* mRNA. The expression levels from untreated cells (-, Control) were set to 100%. Data are the mean ± SEM of three independent experiments made in triplicates.

3.4. Influence of temperature on skin structure

The thermal damage to the skin tissue was further evaluated. When skin is exposed to temperatures above the physiological temperature over an extended period of time, skin tissue damage can occur.[35] We have recently demonstrated that heating rGO loaded hydrogels in contact with a skin at a laser power density of up to 5 W cm^{-2} did not induce any significant histological changes to the skin.[6] **Figure 7** shows the histological analysis of human skin in contact with rGO-COOH/metformin gel before and after laser irradiation (10 min, 0.5-1.0 W cm^{-2}) using conventional haemotoxylin and eosin (H&E) staining. At a laser power density up to 0.7 W cm^{-2} (corresponding to 52°C) normal dermis characteristics are observed. The epidermis as well as the dermis are unaffected. These results are in agreement with reports by others using Cu_7S_4 loaded microneedles, where tissue necrosis in the dermis could be visualized after NIR irradiation for 3 min and 1 min, respectively.[4] Application of ≥ 1 W cm^{-2} laser power results however in skin damage.

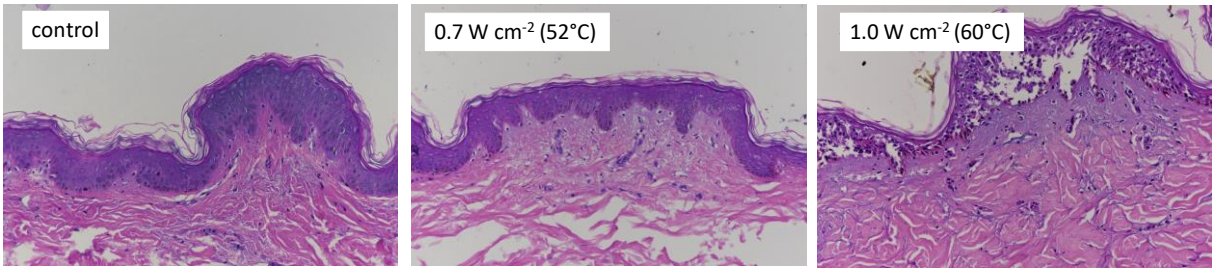

Figure 7: Bright-field micrograph of histological section of an *ex vivo* human skin model before (control) and after 10 min laser irradiation at 0.7 W cm^{-2} and 1 W cm^{-2}.

3.4. *In vivo* studies

Animals were separated into four groups. In the negative control group animals received CMC (0.5 %) *via* oral gavage. The second groups received CMC (0.5 %)/metformin (**Figure 8**) orally in the same manner as the negative group. The third group was composed of animals where metformin (200 mg/kg) was subcutaneously injected. These results were compared to the fourth group treated with rGO-COOH/metformin gels (1 g metformin loading) and being activated for 10 min at 0.7 W cm^{-2}. As seen from the plasma profile in **Figure 8**, a maximal concentration was detected after 30 min when administered orally and under subcutaneous injection. Using the metformin based rGO/COOH patch for the delivery of metformin *via* photothermal activation for 10 min, a maximal plasma concentration was detected after 1h activation where a concentration of 13±2 µg mL^{-1} was detected, in line with other reports.[24] It decreased thereafter slowly until the 2h endpoint.

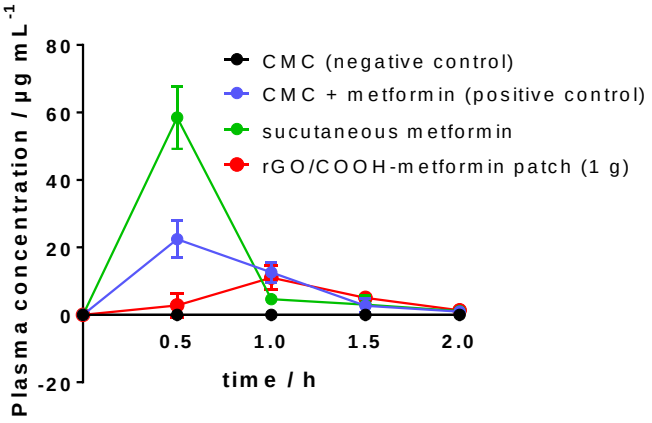

Figure 8: *In vivo* plasma profiles of metformin following oral administration with only CMS (black) or CMS+metformin (blue), subcutaneous metformin injection (green) and following application of the rGO/metformin gel and activation for 10 min at 0.7 W cm^{-2}. n=3 per group.

4. Conclusion

In this study, we presented a novel formulation of a metformin releasing hydrogel based on a simple and straightforward mixing of carboxyl enriched reduced graphene oxide (rGO-COOH) with metformin hydrochloride. Delivery of the antidiabetic drug was achieved by weakening the gelation forces through photothermal heating. The proposed delivery system could release metformin in an intermittent cycle administration with near-infrared light on/off cycles, which increased release in the laser on state. Using mice skin as *ex vivo* model in Franzen diffusion cells, these supramolecular drug reservoirs could deliver transdermally 319±8 µg cm^{-2} (64%,1 W cm^{-2}) and 222±10 µg cm^{-2} (45%, 0.7 W cm^{-2}) in a day, with about 5-30 µg (5-6 %) of metformin being trapped in the skin. *In vitro* assessment of the key target Glucose-6 Phosphatase (G6P) gene expression using Human hepatocyte model confirmed further that the biological activity of metformin remained unaffected by photothermal activation. *In vivo* studies indicated in addition the rise in metformin plasma level, 1h after patch activation.

Acknowledgements

Financial supports from the Centre National de la Recherche Scientifique (CNRS), the University Lille, the Hauts-de-France region, the CPER “Photonics for Society”, the Agence National de la Recherche (ANR) through FLAG-ERA JTC 2015-Graphtivity, and the EU union through the Marie Sklodowska-Curie action (H2020-MSCA-RISE-2015, PANG-690836) are

acknowledged. The Fonds Européen de Développement Régional (FEDER), CNRS, Région Nord Pas-de-Calais and Ministère de l'Education Nationale de l'Enseignement Supérieur et de la Recherche are acknowledged for funding of XPS/LEIS/ToF-SIMS spectrometers within the Pôle Régional d'Analyses de Surface."

References

1. S. Mura, J. Nicolas and P. Couvreur, Stimuli-responsice nanocarriers for drug delivery. *Nat. Materials*, 2013, **12**, 991-1003.
2. C. S. Linsley and B. M. Wu, Recent advances in light-responsive on-demand drug-delivery systems. *Ther Deliv.*, 2017, **8**, 89–107.
3. M. Qiu, D. Wang, L. Liu, Y. Zhang, X. Chen, D. K. Sang, C. Xing, Z. Li, B. Dong, F. Xing, D. Fan, S. Bao, H. Zhang and Y. Cao, Novel concept of the smart NIR-light-controlled drug release of black phosphorus nanostructure for cancer therapy. *Proc Natl Acad Sci U S A.* , 2018, **1145**, 501-506.
4. Y. Zhang, D. Wang, M. Gao, B. Xu, J. Zhu, W. Yu, D. Liu and G. Jiang, Separable Microneedles for Near-Infrared Light-Triggered Transdermal Delivery of Metformin in Diabetic Rats. *ACS Biomater. Sci. Eng.*, 2018, **4**, 2879-2888.
5. L. Zhang, Y. Li, Z. Jin, J. C. Yu and K. M. Chan, An NIr-triggered and thermally responsive drug delivery platfrom through DNA/copper sulfide gates. *Nanoscale*, 2015, **7**, 12614.
6. F. Teodorescu, G. Guéniat, C. Foulon, M. Lecoeur, A. Barras, S. Boulahneche, M. S. Medjram, T. Hubert, A. Abderrahmani, R. Boukherroub and S. Szunerits, Transdermal skin patch based on reduced graphene oxide: A new approach for photothermal triggered permeation of ondansetron across porcine skin. *J. Control. Release*, 2017, **245**, 137-146.
7. F. Teodurescu, Y. Oz, G. Quéniat, A. Abderrahmani, C. Foulon, M. Lecoeur, R. Sanyal, A. Sanyal, R. Boukherroub and S. Szunerits, Photothermally triggered on-demand insulin release from reduced graphene oxide modified hydrogels. *J. Control. Release*, 2017, **246**, 164-173.
8. I. Altinbasak, R. Jijie, A. Barras, B. Golba, R. Sanyal, J. Bouckaert, D. Drider, R. Bilyy, T. Dumych, S. Paryzhak, V. Vovk, R. Boukherroub, A. Sanyal and S. Szunerits, Reduced Graphene-Oxide-Embedded Polymeric Nanofiber Mats: An "On-Demand" Photothermally Triggered Antibiotic Release Platform. *ACS Appl. Mater. Interfaces*, 2018, **10**, 41098-41106.
9. P. Zhao, M. Zheng, Z. Luo, P. Gong, G. Gao, Z. Sheng, C. Zheng, Y. Ma and L. Cai, NIR-driven Smart Theranostic Nanomedicine for On-demand Drug Release and Synergistic Antitumour Therapy. *Sci Rep.*, 2015, **5**, 14258.
10. J. Lu, S. Zhang, L. Guo and W. Li, Applications of graphene-based composite hydrogels: a review *RSC Adv.*, 2017, **7**, 51008-51020.
11. G. Liao, J. Hu, Z. Chen, R. Zhang, G. Wang and T. Kuang, Preparation, Properties, and Applications of Graphene-Based Hydrogels. *Front. Chem.*, 2018, **6**, 450.
12. Y. Xu, K. Sheng, S. Li and G. Shi, Self-Assembled Graphene Hydrogel via a One-Step Hydrothermal Process. *ACS Nano*, 2010, **4**, 4324-4330.
13. Z. Fan, B. Liu, J. Wang, S. Zhang, Q. Lin, P. Gong, L. Ma and S. Yang, A Novel Wound Dressing Based on Ag/Graphene Polymer Hydrogel: Effectively Kill Bacteria and Accelerate Wound Healing. *Adv. Funct. Mater.*, 2014, **24**, 3933-3943.
14. P. W. Gong, S. J. Ji, J. Q. Wang, D. J. Dai, F. Wang, M. Tian, L. Zhang, F. F. Guo and Z. Liu, Fluorescence-switchable ultrasmall fluorinated graphene oxide with high near-

infrared absorption for controlled and targeted drug delivery. *Chem. Eng. J.*, 2018, **348**, 438-446.
15. C.-A. Tao, J. Wang, S. Qin, Y. Lv, Y. Long, H. Zhua and Z. Jianga, Fabrication of pH-sensitive graphene oxide–drug supramolecular hydrogels as controlled release systems. *J. Mater. Chem.* , 2012, **22**, 2485-24861.
16. M.-C. Chen, Z.-W. Lin and M.-H. Ling, Near-Infrared Light-Activatable Microneedle System for Treating Superficial Tumors by Combination of Chemotherapy and Photothermal Therapy. *ACS Nano*, 2016, **10**, 93-101.
17. S. Szunerits and R. Boukherroub, Heat: A Highly Efficient Skin Enhancer for Transdermal Drug Delivery. *Front. Bioeng. Biotechnol.*, **6**, 15.
18. J. Yu, Y. Zhang, A. R. Kahkoska and Z. Gu, Bioresponsive transcutaneous patches. *Curr. Opin. Biotechnol.*, 2017, **48**, 28-32.
19. M. N. Pastore, Y. N. Kalia, M. Horstmann and M. S. Roberts, Transdermal patches: history, development and pharmacology. *Brit. J. Pharmacol.*, 2015, **172**, 2179-2209.
20. B. Viollet, B. Guigas, N. Sanz Garcia, J. Leclerc, M. Foretz and F. Andreelli, Cellular and molecular mechanisms of metformin: an overview. *Clin. Sci. (Lond)*, 2012, **122**, 253-270.
21. Graham, G. G. Graham, J. Punt, M. Arora, R. O. Day, M. P. Doogue, J. K. Duong, T. J. Furlong, J. R. Greenfield, L. C. Greenup, C. M. Kirkpatrick, J. E. Ray, P. Timmins and K. M. Williams, Clinical pharmacokinetics of metformin. *Clin. Pharmacokinet.*, 2011, **50**, 81-98.
22. Y. Zhang, G. Jiang, W. Hong, M. Gao, B. Xu, J. Zhu, G. Song and T. Liu, Polymeric Microneedles Integrated with Metformin-Loaded and PDA/LA-Coated Hollow Mesoporous SiO2 for NIR-Triggered Transdermal Delivery on Diabetic Rats. *ACS Appl. Bio Mater.*, 2018, **1**, 1906–1917.
23. X. Yu, Y. Jin, L. Du, M. Sun, J. Wang, Q. Li, X. Zhang, Z. Gao and P. Ding, Transdermal Cubic Phases of Metformin Hydrochloride: In Silico and in Vitro Studies of Delivery Mechanisms. *Mol. Phamaceutics*, 2018, **15**, 3121-3132.
24. E. M. Migdadi, A. J. Courtenay, I. A. Tekko, M. T. C. McCrudden, M. C. Kearney, E. McAlister, H. O. McCarthy and R. F. Donnelly, Hydrogel-forming microneedles enhance transdermal delivery of metformin hydrochloride. *J. Control Release*, 2018, **285**, 142-151.
25. W. Yu, G. Jiang, Y. Zhang, D. Liu, B. Xu and J. Zhou, Near-infrared light triggered and separable microneedles for transdermal delivery of metformin in diabetic rats *J. Mater. Chem. B*, 2017, **5**, 9507-9513
26. H. Lee, T. K. Choi, Y. B. Lee, H. R. Cho, R. Ghaffari, L. Wang, H. J. Choi, T. D. Chung, N. Lu, T. Hyeon, S. H. Choi and D.-H. Kim, A graphene-based electrochemical device with thermoresponsive microneedles for diabetes monitoring and therapy. *Nat. Nanotechnol.*, 2016, **11**, 566-572.
27. J. Li and D. J. Mooney, Designing hydrogels for controlled drug delivery. *Nat. Rev. Mater.*, 2016, **1**, 16071
28. A. Abderrahmani, L. Yengo, R. Caiazzo, M. Canouil, S. Cauchi, V. Raverdy, V. Plaisance, V. Pawlowski, S. Lobbens, J. Maillet, L. Rolland, R. Boutry, G. Queniat, M. Kwapich, M. Tenenbaum, J. Bricambert, S. Saussenthaler, E. Anthony, P. Jha, J. Derop, O. Sand, I. Rabearivelo, A. Leloire, M. Pigeyre, M. Daujat-Chavanieu, S. Gerbal-Chaloin, T. Dayeh, G. Lassailly, P. Mathurin, B. Staels, J. Auwerx, A. Schürmann, C. Postic, C. Schafmayer, J. Hampe, A. Bonnefond, F. Pattou and P. Froguel, Increased Hepatic PDGF-AA Signaling Mediates Liver Insulin Resistance in Obesity-Associated Type 2 Diabetes. *Diabetes*, 2018, **67**, 1310-1321.
29. A. Madsen, O. Bozickovic, J. I. Bjune, G. Mellgren and J. V. Sagen, Metformin inhibits hepatocellular glucose, lipid and cholesterol biosynthetic pathways by

transcriptionally suppressing steroid receptor coactivator 2 (SRC-2). *Sci Rep.* , 2015, **5**, 16430.
30. X. Sun, Z. Liu, K. Welsher, J. T. Robinson, A. Goodwin, S. Zaric and H. Dai, Nano-Graphene Oxide for Cellular Imaging and Drug Delivery. *Nano Res.* , 2008, 203.
31. K. Turcheniuk, C.-H. J. Hage, Spadavecchia, A. Yanguas Serrano, I. Larroulet, A. Pesquera, A. Zurutuza, M. Gonzales Pisfil, L. Heliot, J. Bouckaert, R. Boukherroub and S. Szunerits, Plasmonic photothermal destruction of uropathogenic E. coli with reduced graphene oxide and core/shell nanocomposites of gold nanorods/reduced graphene oxide. *J. Mater. Chem B*, 2015, **3**, 375-386
32. Q. Lai, Shifu Zhu, Xueping Luo, Min Zou and S. Huang, Ultraviolet-visible spectroscopy of graphene oxides. *AIP Advances*, 2012, **2**, 032146
33. P. Gong, J. Du, D. Wng, B. Cao, M. Tian, Y. Wang, L. Sun, S. Ji and Z. Liu, Fluorinated graphene as an anticancer nanocarrier: an experimental and DFT study. *J. Mater. Chem. B*, 2018, **6**, 2769-2777
34. K. Yang, J. Wan, S. Zhang, B. Tian, Y. Zhang and Z. Liu, The influence of surface chemistry and size of nanoscale graphene oxide on photothermal therapy of cancer using ultra-low laser power. *Biomaterials*, 2012, **33**, 2206-2214.
35. I.-T. Im, S. B. Youn and K. Kim, Numerical Study on the Temperature Profiles and Degree of Burns in Human Skin Tissue During Combined Thermal Therapy. *Numer. Heat Transfer, Part A*, 2015, **67**, 921-933.